

Electronic supplementary information (ESI)

Thieno[3,2-b]indole-based hole transporting materials for perovskite solar cells with photovoltages exceeding 1.11 V

Liyuan Liu,^a Yungen Wu,^a Mengyuan Li,^a Xueping Zong,^{*a} Zhe Sun,^a Mao Liang^{*a,b} and
Song Xue^a

^a Tianjin Key Laboratory of Organic Solar Cells and Photochemical Conversion, Department of Applied Chemistry, Tianjin University of Technology, Tianjin 300384, P. R. China.

^b Key Laboratory of Advanced Energy Materials Chemistry (Ministry of Education), Collaborative Innovation Center of Chemical Science and Engineering, College of Chemistry, Nankai University, Tianjin 300071, P. R. China.

Email: liangmao717@126.com;

Email: zongxueping717@163.com

List of contents

1	Base characterization of HTMs	S1-4
2	Device fabrication	S4-6
3	Photovoltaic performance characterizations	S6-7
4	Synthetic procedures	S7-13
5	Table S1-3	S15
6	$^1\text{H}/^{13}\text{C}$ NMR spectra of new compounds (Fig. S1-9)	S16-24
7	Fig. S10-21	S25-31
8	References	S32-33

1. Base Characterization of HTMs

1.1 Uv-vis and DPV measurements.

The absorption spectra of the solution of HTMs (dissolve in THF) were measured by SHIMADZU UV-2600 spectrophotometer. Same samples of fluorescence measurements were recorded by a HITACHI F-4500 fluorescence spectrophotometer. Differential pulse voltammetry (DPV) of these samples containing 0.1 M of tetrabutylammoniumhexafluorophosphate (n-Bu₄NPF₆) were performed on a CHI660D electrochemical workstation in conjunction with a three-electrode electrochemical cell composed of a platinum electrode (counter electrode), Ag/AgCl electrode (reference electrode) and a glassy carbon disk (working electrode) at a scan rate of 50 mV s⁻¹. All potentials were reported against the ferrocene/ferrocenium (Fc/Fc⁺) reference.

1.2 Mobility Measurements

Hole mobility of the studied HTMs were recorded by space-charge-limited currents (SCLCs) method, which can be described by the Mott-Gurney equation^{1,2}:

$$J = 9\mu\epsilon_0\epsilon_r V^2 / (8d^3)$$

where J is the current density, μ is the hole mobility, ϵ_0 is the vacuum permittivity (8.85*10⁻¹² F/m), ϵ_r is the dielectric constant of material (normally taken to approach 3 for organic semiconductors), V is the applied bias, and d is the film thickness.

First, PEDOT: PSS was spin coated onto the substrates and then annealed on a hotplate at 120 °C for 30 min, forming a thin layer (< 100 nm). After that, HTMs (without dopant) was deposited via spin-coating at 2000 rpm for 30 s. Finally, a 150

nm thick Ag back contact was deposited onto the HTM layer. The thicknesses of the HTMs were measured by using a Dektak profilometer. The current density of devices has been measured with a Keithley 2400 Source-Measure unit.

1.3 Quantum chemical calculation

Quantum chemical calculation was performed on the Gaussian 09 software package³. We optimized the molecular structure of M107-110 at the B3LYP/6-31G level in the vacuo.

2. Device Fabrication

2.1 Materials

FAI, MABr, mesoporous TiO₂ (30 NRD) and FK209 were purchased from Greatcellsolar (Australia). PbI₂, PbBr₂ and CsI were purchased from TCI. Fluorine doped tin dioxide (FTO) coated glass substrates were purchased from Hartford Glass Company. Spiro-MeOTAD was purchased from p-OLED (China). Lithium bis-(trifluoromethylsulfonyl)imide obtained from Sigma Aldrich. The SnO₂ colloid precursor was obtained from Alfa Aesar (tin (IV) oxide).

2.2 Fabrication

Perovskite solar cells were fabricated on fluorine-doped tin dioxide (FTO) coated substrates (1.5 cm × 2.0 cm). FTO substrates were etched by diluted HCl solution (1 ml HCl in 10 ml DI water) and Zinc powder. The etched substrates were then cleaned via sonication in soap water, DI-water, acetone and isopropanol for 25 min, respectively, followed by treatment with oxygen plasma.

The electron transport layer (SnO₂) was prepared according to the method reported by a previously work.⁴ The substrate was spin coated with a thin layer of SnO₂

nanoparticle film (2.67%) at 4000 rpm for 30 s, and annealed in ambient air at 150 °C for 30 min. The PCBM layer (10 mg mL⁻¹ in chlorobenzene) was deposited on the prepared SnO₂ layer by spin-coating at 3000 rpm for 30 s and 4000 rpm for 5 s.

Perovskite film was prepared according to the method reported by a previously work.⁵ The “mixed” perovskite precursor solutions were deposited from a precursor solution containing FAI/PbI₂/MABr/PbBr₂ (mole ratio is 1/1.1/0.2/0.2) in anhydrous DMF/DMSO (v/v = 4/1). To improve the quality of perovskite film, CsI (1.5 M) was added to the above solution. The volume ratio of FAI/PbI₂/MABr/PbBr₂ and CsI is 95 / 5. The mixed solution was stirred under 60 °C for half of an hour. A two steps program at 1000 and 6000 rpm for 10 and 30 s respectively was employed for spin. During the second step, 100 μL of chlorobenzene was poured on the spinning substrate 15s prior to the end of the program. Films with Cs-containing perovskite turned dark immediately after spin coating. The substrates were then annealed (usually at 100 °C) for 1 h in a nitrogen filled glove box.

After the perovskite annealing, the substrates were cooled down for few minutes and a solution (chlorobenzene) of HTMs (Spiro-OMeTAD, 70 mM; M107-110, 60 mM) was spin coated at 4000 rpm for 20 s. In addition, the solution was doped with Li-TFSi and FK209 and TBP. The molar ratio of additives for HTM was 0.5, 0.03 and 3.3 for Li-TFSi, FK209 and TBP, respectively. Samples were then transferred to the evaporator for Au deposition (80 nm) as the top electrode.

3. Photovoltaic Performance Characterizations

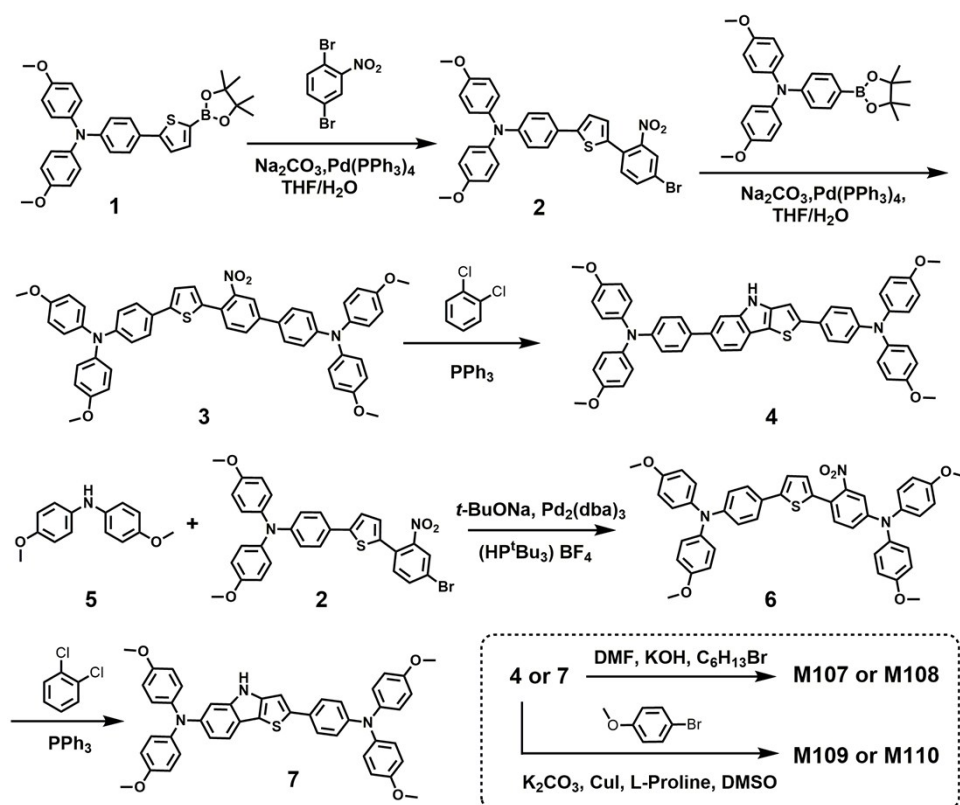
The current density–voltage ($J-V$) characterization of the devices was carried out

by using a standard xenon-lamp-based solar simulator (Oriel Sol 3A, USA) under simulated AM 1.5 irradiation ($100 \text{ mW}\cdot\text{cm}^{-2}$) with a digital source meter (Keithley 2400). The $J-V$ measurement was carried out under reverse scan with a scan rate of 0.1 V/s . At the same time, a measurement under forward scan was also performed for the devices to check the hysteresis of the $J-V$ curve. A monocrystalline silicon reference cell (Oriel P/N 91150 V, with KG-5 visible color filter) calibrated by the National Renewable Energy Laboratory (NREL) was used to confirm the solar simulator illumination intensity. All tests were carried out in air, and a mask with defined area size of 14.0 mm^2 was attached onto the cell during test. Dozens of devices were fabricated and measured independently to obtain the statistical histograms of PCE devices. The action spectra of monochromatic incident photon-to-current conversion efficiency (IPCE) for solar cell were performed by using a commercial setup (QTest Station 2000 IPCE Measurement System, CROWNTech, USA).

4. Synthetic procedures

4.1 Materials and Instruments

$\text{Pd}(\text{PPh}_3)_4$, $\text{Pd}_2(\text{dba})_3$, $t\text{-BuONa}$, $n\text{-butyllithium}$, PPh_3 , CuI , $(\text{HP}^t\text{Bu}_3)\text{BF}_4$, CuI and $L\text{-proline}$ were purchased from Energy Chemical (China). ^1H and ^{13}C NMR spectra were recorded on a Bruker AM-300 or AM-400 spectrometer. The reported chemical shifts were against TMS. High-resolution mass spectra (HRMS) were obtained with a Micromass GCT-TOF mass spectrometer. The melting point (MP) was taken on a RY-1 thermometer, and temperatures were uncorrected.



Scheme S1. Synthetic routes for M107-110

The synthetic routes of M107-110 are shown in Scheme S1 and the preparation details are described as follows.

4.2 Synthesis of compound 2

To a 100 mL two-neck round-bottom flask, a solution of compound **1** (2.0 g, 3.9 mmol), 2,5-dibromonitrobenzene (1.64 g, 5.84 mmol), Pd(PPh₃)₄ (0.045 g, 0.04 mmol), and 7.8 mL of K₂CO₃ (an aqueous solution(2 M) of K₂CO₃) in 30 mL of anhydrous THF was stirred at 90 °C under nitrogen atmosphere. The mixture was refluxed for 8 hours. After cooling to room temperature, the crude mixture was extracted with 100mL of DCM and washed with 100 mL of water. THF was evaporated under reduced pressure. The mixture dried over Na₂SO₄ and the remaining

crude product was purified by column chromatography on silica gel eluted using DCM/PE (1: 10 by volume) as eluent. Compound **2** (red oil, 1.96 g, 85.6% yield). IR (KBr): 3696, 2936, 2866, 2356, 1725, 1561, 1076, 973, 860, 739, 678 cm^{-1} . ^1H NMR (400 MHz, CDCl_3) δ 7.88 (s, 1H), 7.71 (dd, $J = 8.4, 2.0$ Hz, 1H), 7.48 (d, $J = 8.4$ Hz, 1H), 7.41 (d, $J = 8.4$ Hz, 2H), 7.15 (d, $J = 3.9$ Hz, 1H), 7.10 (d, $J = 8.4$ Hz, 4H), 7.04 (d, $J = 3.8$ Hz, 1H), 6.93 (d, $J = 8.3$ Hz, 2H), 6.87 (d, $J = 8.6$ Hz, 4H), 3.83 (s, 6H). ^{13}C NMR (101 MHz, CDCl_3) δ 156.17, 149.25, 148.82, 147.27, 140.44, 134.93, 133.40, 132.97, 128.44, 127.32, 126.85, 126.56, 125.39, 122.46, 121.21, 120.14, 114.81, 55.51. HRMS (EIS) caclcd for $\text{C}_{30}\text{H}_{24}\text{BrN}_2\text{O}_4\text{S}$ ($\text{M}+\text{H}^+$): 587.0640, found: 587.0642.

4.3 Synthesis of compound **3**

A mixture of compound **2** (1.96 g, 3.34 mmol), compound **9** (2.16 g, 0.5 mmol), and $\text{Pd}(\text{PPh}_3)_4$ (0.039 g, 0.033 mmol), were added into a 100 mL two-neck round bottom flask under a nitrogen atmosphere. THF (20 mL) was then added. Aqueous sodium carbonate solution (2 M, 6.7 mL) was added and the reaction mixture was stirred at 80 °C for 12 h. The reaction mixture was extracted by dichloromethane (3 \times 20 mL). The combined organic extract was washed with water and dried over MgSO_4 . The crude product was purified by employing silica gel column chromatography using EA/DCM/PE (1:20:100 by volume) as the eluent. The product was collected as a red oil (1.9 g, 70% yield). IR (KBr): 3472, 2365, 2321, 1639, 1569, 1371, 1215, 1025, 835, 679, 575, 471 cm^{-1} . ^1H NMR (400 MHz, CDCl_3) δ 7.89 (s, 1H), 7.73 (d, $J = 8.2, 2.0$ Hz, 1H), 7.61 (d, $J = 8.2$ Hz, 1H), 7.44 (ddd, $J = 8.5, 5.1, 2.1$ Hz, 4H), 7.13

(tt, $J = 8.9, 3.4$ Hz, 9H), 7.06 (d, $J = 3.8$ Hz, 1H), 7.01 (d, $J = 8.5$ Hz, 2H), 6.95 (d, $J = 8.9, 2.6$ Hz, 2H), 6.91–6.86 (m, 8H), 3.84 (s, 12H). ^{13}C NMR (101 MHz, CDCl_3) δ 156.34, 156.11, 149.50, 149.37, 148.61, 146.45, 141.21, 140.57, 140.33, 134.88, 132.08, 129.18, 129.13, 128.49, 127.92, 127.40, 127.05, 126.77, 126.52, 125.84, 125.73, 122.42, 121.31, 120.3, 120.02, 114.88, 114.80, 55.52. HRMS (EIS) cacl'd for $\text{C}_{50}\text{H}_{42}\text{N}_3\text{O}_6\text{S}(\text{M}+\text{H}^+)$: 812.2794, found: 812.2794.

4.4 Synthesis of compound 6

Dissolve bis(panisyl)amine (compound **5**, 1.2 g, 5.23 mmol), compound **2** (2.05 g, 3.49 mmol), *t*-BuONa (1.34 g, 13.96 mmol), $\text{Pd}_2(\text{dba})_3$ (0.16 g, 0.174 mmol) and $(\text{HP}^t\text{Bu}_3)\text{BF}_4$ (0.051 g, 0.193 mmol) with dry toluene (25 mL) in a 100 mL two-neck round-bottom flask. Heat the reaction mixture to reflux under N_2 overnight. After evaporating the solvent under reduced pressure, the crude product was purified by employing silica gel column chromatography using EA/DCM/PE (1:20:100 by volume) as the eluent. The product was collected as a red oil (1.03 g, 40.2% yield). IR (KBr): 3489, 2927, 1612, 1552, 1500, 1344, 1310, 1231, 1163, 1042, 860, 782, 600, 540, 454 cm^{-1} . ^1H NMR (400 MHz, CDCl_3) δ 7.38 (d, 2H), 7.29 (d, $J = 8.6$ Hz, 1H), 7.15–7.10 (m, 5H), 7.10–7.05 (m, 5H), 6.99 (d, $J = 8.7, 2.5$ Hz, 1H), 6.94–6.87 (m, 7H), 6.87–6.82 (m, 4H), 3.81 (d, $J = 6.1$ Hz, 12H). ^{13}C NMR (101 MHz, CDCl_3) δ 157.14, 156.06, 149.86, 148.98, 148.41, 145.34, 140.65, 138.99, 135.61, 132.20, 127.45, 127.06, 126.69, 126.43, 126.16, 122.25, 120.82, 120.48, 118.19, 115.24, 112.66, 55.52, 55.51. HRMS (EIS) cacl'd for $\text{C}_{44}\text{H}_{38}\text{N}_3\text{O}_6\text{S}(\text{M}+\text{H}^+)$: 736.2481, found: 736.2480.

4.5 Synthesis of compound 4/7

A mixture of compound **3/6** (1.9 g, 2.34 mmol/1.03 g, 1.4 mmol) and triphenylphosphine (1.84 g, 7.02 mmol/1.1 g, 4.2 mmol) in 30 mL of dry chlorobenzene was refluxed at 180 °C under nitrogen for over 16 hours. After evaporating the solvent under reduced pressure, the crude product was purified by column chromatography on silica gel eluted with EA/DCM/PE (1:10:50 by volume) to afford the product compound **4/7** (yellow solid, 1.09 g/0.591 g, 60% yield).

Compound **4**, MP: 112-114 °C. IR (KBr): 3493, 3482, 3473, 2925, 2833, 1610, 1432, 1400, 1340, 1310, 1230, 1100, 1089, 1042, 880, 780, 600, 550, 447 cm⁻¹. ¹H NMR (400 MHz, DMSO-*d*₆) δ 11.43 (s, 1H), 7.69 (d, *J* = 8.2 Hz, 1H), 7.62 (s, 1H), 7.56 (dd, *J* = 8.5, 3.4 Hz, 4H), 7.44 (s, 1H), 7.34 (d, *J* = 7.9 Hz, 1H), 7.07 (dd, 8H), 6.94 (dd, *J* = 8.9, 3.1 Hz, 8H), 6.87 (d, *J* = 8.3 Hz, 2H), 6.81 (d, *J* = 8.3 Hz, 2H), 3.76 (s, 12H). ¹³C NMR (101 MHz, THF-*d*₈) δ 156.38, 156.11, 155.92, 155.81, 141.85, 141.73, 141.19, 141.11, 141.07, 140.64, 127.29, 127.17, 126.48, 126.45, 126.17, 126.06, 125.90, 125.83, 125.77, 121.10, 121.02, 120.42, 120.37, 114.54, 114.46, 114.34, 54.65. HRMS (EIS) calcd for C₅₀H₄₂N₃O₄S (M+H⁺): 780.2896, found: 780.2899.

Compound **7**, MP: 90-91 °C. IR (KBr): 3502, 3479, 3473, 2899, 2843, 1672, 2643, 1432, 1400, 1340, 1310, 1230, 1100, 1067, 1042, 880, 787, 622, 552, 419 cm⁻¹. ¹H NMR (400 MHz, DMSO-*d*₆) δ 11.09 (s, 1H), 7.52 (dd, *J* = 12.5, 8.5 Hz, 3H), 7.38 (s, 1H), 7.06 (d, *J* = 8.6 Hz, 5H), 6.98 (d, *J* = 8.7 Hz, 4H), 6.94 (d, *J* = 8.7 Hz, 3H), 6.91–6.87 (m, 5H), 6.79 (d, *J* = 8.4 Hz, 2H), 6.72–6.66 (m, 1H), 3.75 (dd, *J* = 7.6, 1.4 Hz,

12H). ^{13}C NMR (101 MHz, THF- d_8) δ 156.74, 154.49, 146.42, 140.26, 138.72, 129.50, 125.14, 124.55, 124.39, 123.88, 123.26, 118.55, 116.73, 115.97, 115.51, 112.87, 112.74, 112.64, 112.37, 103.35, 52.88, 52.77. HRMS (EIS) calcd for $\text{C}_{44}\text{H}_{38}\text{N}_3\text{O}_4\text{S}$ ($\text{M}+\text{H}^+$): 704.2583, found: 704.2585.

4.6 Synthesis of compound M107

A solution of compound **4** (1.09 g, 1.4 mmol), potassium hydroxide (0.314 g, 5.6 mmol) in 15 mL of DMSO was stirred at room temperature for 30 minutes. 1-bromo-hexane (0.277 g, 1.68 mmol) was poured into the mixture. The reaction was stirred for 8 hours at room temperature. The reaction mixture was filtered, and the solvent was evaporated under reduced pressure. The crude product was purified on silica gel chromatography using EA/DCM/PE (3:20:100 by volume) as eluent to afford a yellow solid (0.792 g, 65.6% yield). MP: 113-114 °C. IR (KBr): 3480, 2927, 2365, 2338, 1656, 1491, 1250, 1189, 1025, 835, 713, 584 cm^{-1} . ^1H NMR (400 MHz, DMSO- d_6) δ 7.75 (s, 1H), 7.70 (d, $J = 8.3$ Hz, 1H), 7.66–7.52 (m, 5H), 7.35 (d, $J = 8.8$ Hz, 1H), 7.10–7.02 (m, 8H), 6.94 (dt, $J = 8.9, 2.9$ Hz, 8H), 6.86 (dd, $J = 27.4, 8.3$ Hz, 4H), 4.40 (t, 2H), 3.76 (s, 12H), 1.81 (s, 2H), 1.26 (d, $J = 17.4$ Hz, 6H), 0.81 (t, $J = 6.7$ Hz, 3H). ^{13}C NMR (101 MHz, THF- d_8) δ 155.95, 155.65, 147.93, 147.27, 145.86, 145.13, 141.16, 140.66, 140.17, 134.69, 134.17, 127.35, 126.95, 126.04, 125.67, 125.42, 120.74, 120.42, 119.94, 117.83, 117.62, 114.09, 114.00, 113.29, 106.84, 104.79, 54.20, 44.17, 31.17, 29.35, 26.30, 22.09, 13.00. HRMS (EIS) calcd for $\text{C}_{56}\text{H}_{54}\text{N}_3\text{O}_4\text{S}$ ($\text{M}+\text{H}^+$): 864.3835, found: 864.3835.

4.7 Synthesis of compound M108

Compound **M108** was synthesized from **M107** according to the same procedure in compound **4**. 1-bromo-hexane was used as a starting material, giving **M108** as a yellow solid (54.2% yield). MP: 69-70 °C. IR (KBr): 4372, 2953, 2357, 1639, 1500, 1232, 1171, 1103, 1042, 826, 670, 514, 402 cm⁻¹. ¹H NMR (400 MHz, DMSO-*d*₆) δ 7.58 (s, 1H), 7.53 (dd, *J* = 8.7, 1.8 Hz, 3H), 7.06 (d, 4H), 6.99–6.92 (m, 9H), 6.88 (d, 4H), 6.81 (d, *J* = 8.7 Hz, 2H), 6.69 (dd, *J* = 8.5, 1.9 Hz, 1H), 4.14 (t, 2H), 3.75 (d, *J* = 9.8 Hz, 12H), 1.66 (t, 2H), 1.24 (s, 6H), 0.81–0.76 (m, 3H). ¹³C NMR (101 MHz, THF-*d*₈) δ 156.33, 155.40, 148.17, 144.30, 140.68, 126.35, 125.68, 125.04, 120.57, 118.47, 117.52, 116.22, 114.50, 114.23, 104.45, 54.63, 54.58, 44.36, 31.48, 29.64, 26.55, 22.40, 13.37. HRMS (EIS) caclcd for C₅₀H₅₀N₃O₄S (M+H⁺): 788.3522, found: 788.3520.

4.8 Synthesis of compound **M109**

Equip a 100 mL, two-necked round-bottom flask with a mixture of 4-iodoanisole (0.49 g, 2.1 mmol), compound **4** (1.09 g, 1.4 mmol), K₂CO₃ (2.32 g, 16.8 mmol), CuI (0.0133 g, 0.07 mmol), L-proline (0.032 g, 0.28 mmol) in 10 mL of DMSO at 90 °C under nitrogen atmosphere for 40 h. After cooling to room temperature, the crude mixture was extracted with DCM and washed with 5×20 mL of water. The crude product was purified on silica gel chromatography using EA/DCM/PE (1:5:25 by volume) as eluent to afford a yellow solid (0.51 g, 41.2% yield). MP: 117-120 °C. IR (KBr): 3455, 2919, 2841, 2365, 2313, 1716, 1604, 1509, 1457, 1231, 1180, 1033, 835, 791, 730, 601, 523 cm⁻¹. ¹H NMR (400 MHz, DMSO-*d*₆) δ 7.82 (d, *J* = 8.3 Hz, 1H), 7.63 (d, 2H), 7.57 (d, *J* = 8.3 Hz, 2H), 7.47 (dd, *J* = 20.5, 9.0 Hz, 4H), 7.36 (s, 1H),

7.19 (d, $J = 8.5$ Hz, 2H), 7.08–7.02 (m, 8H), 6.96–6.89 (m, 8H), 6.85 (d, $J = 8.6$ Hz, 2H), 6.78 (d, $J = 8.4$ Hz, 2H), 3.87 (s, 3H), 3.75 (s, 12H). ^{13}C NMR (101 MHz, THF- d_8) δ 157.01, 154.56, 154.23, 146.62, 145.93, 144.43, 144.09, 140.21, 139.17, 138.69, 133.89, 132.40, 129.56, 125.63, 125.42, 124.97, 124.64, 124.23, 124.03, 123.75, 119.27, 118.38, 117.22, 116.44, 113.01, 112.66, 112.57, 106.18, 103.88, 52.96, 52.76. HRMS (EIS) caclcd for $\text{C}_{57}\text{H}_{48}\text{N}_3\text{O}_5\text{S}$ ($\text{M}+\text{H}^+$): 886.3314, found: 886.3315.

4.9 Synthesis of compound M110

M110 was synthesized from **M109** according to the same procedure in compound 7, 4-iodoanisole as a starting material, to give **M110**, as a yellow solid 40.6% yield. MP: 105-106 °C. IR (KBr): 3455, 2849, 2365, 2330, 1612, 1500, 1241, 1171, 1042, 817, 730, 679, 584, 532 cm^{-1} . ^1H NMR (400 MHz, CDCl_3) δ 7.59 (d, $J = 8.6$ Hz, 1H), 7.47 (dd, $J = 6.8, 2.9$ Hz, 2H), 7.42 (d, 2H), 7.17–7.08 (m, 6H), 7.05 (d, $J = 9.2$ Hz, 5H), 7.02 (s, 1H), 6.98–6.93 (m, 3H), 6.87 (d, 4H), 6.82 (d, 4H), 3.89 (s, 3H), 3.82 (d, $J = 8.0$ Hz, 12H). ^{13}C NMR (101 MHz, THF- d_8) δ 156.73, 154.48, 146.43, 140.25, 138.69, 129.49, 128.73, 126.74, 125.74, 124.55, 124.37, 118.52, 116.71, 115.95, 115.49, 112.87, 112.63, 112.35, 103.34, 101.52, 52.87, 52.76, 52.71. HRMS (EIS) caclcd for $\text{C}_{51}\text{H}_{44}\text{N}_3\text{O}_5\text{S}$ ($\text{M}+\text{H}^+$): 810.3001, found: 810.3002.

Table S1. Optical and Electrochemical Properties of M107-110 and X25.

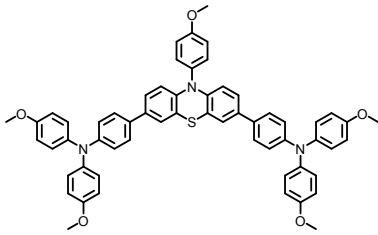
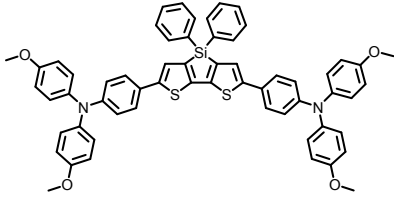
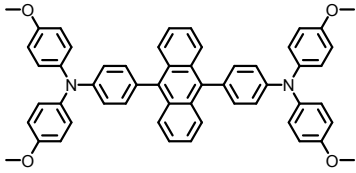
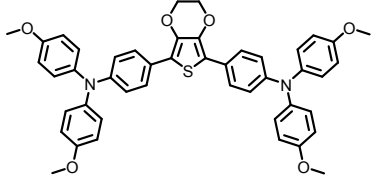
HTMs	$\lambda_{abs}/\text{nm}^a$	$\lambda_{emi}/\text{nm}^b$	E_g/eV^c	HOMO/V vs NHE ^d	LUMO/V vs NHE ^e
M107	405	465	2.786	-5.12	-2.33
M108	410	469	2.758	-5.14	-2.34
M109	403	465	2.798	-4.89	-2.14
M110	412	468	2.765	-4.93	-2.17
X25	333	418	3.221	-5.22	-1.99

The absorption^a and emission^b peak of M107-110 and X25 in THF. ^c E_g is the energy gap between the HOMO and LUMO. ^d HOMO was recorded by DPV of HTMs. ^e LUMO was calculated from HOMO- E_{0-0} .

Table S2. Hole Mobility and T_g of M107-110 and X25.

HTMs	Hole mobility / $\text{cm}^2 \cdot \text{V}^{-1} \cdot \text{s}^{-1}$	$T_g / ^\circ\text{C}$
M107	1.57×10^{-5}	84.43
M108	9.75×10^{-7}	66.69
M109	1.71×10^{-5}	117.65
M110	4.46×10^{-6}	104.39
X25	1.51×10^{-5}	123.73

Table S3. Typical linear HTMs with two bismethoxy substituted triphenylamine groups and electron-rich cores as well as their PCE performance.

HTMs	PCE	References
 <p style="text-align: right;">PTZ-2</p>	17.6%	Grisorio et al. <i>ACS Energy Lett.</i> , 2017, 2, 1029–1034
Spiro-OMeTAD (reference HTM)	17.7%	
 <p style="text-align: right;">PEH-2</p>	13.5%	Abate et al. <i>Energy Environ. Sci.</i> , 2015, 8, 2946--2953.
Spiro-OMeTAD (reference HTM)	15.2%	
 <p style="text-align: right;">A102</p>	16.22%	Liu et al. <i>Chem. Commun.</i> , 2017, 53, 9558--9561
Spiro-OMeTAD (reference HTM)	15.63%	
 <p style="text-align: right;">H101</p>	13.8%	Li et al. <i>Angew. Chem. Int. Ed.</i> 2014, 53, 1 – 5
Spiro-OMeTAD (reference HTM)	13.7%	

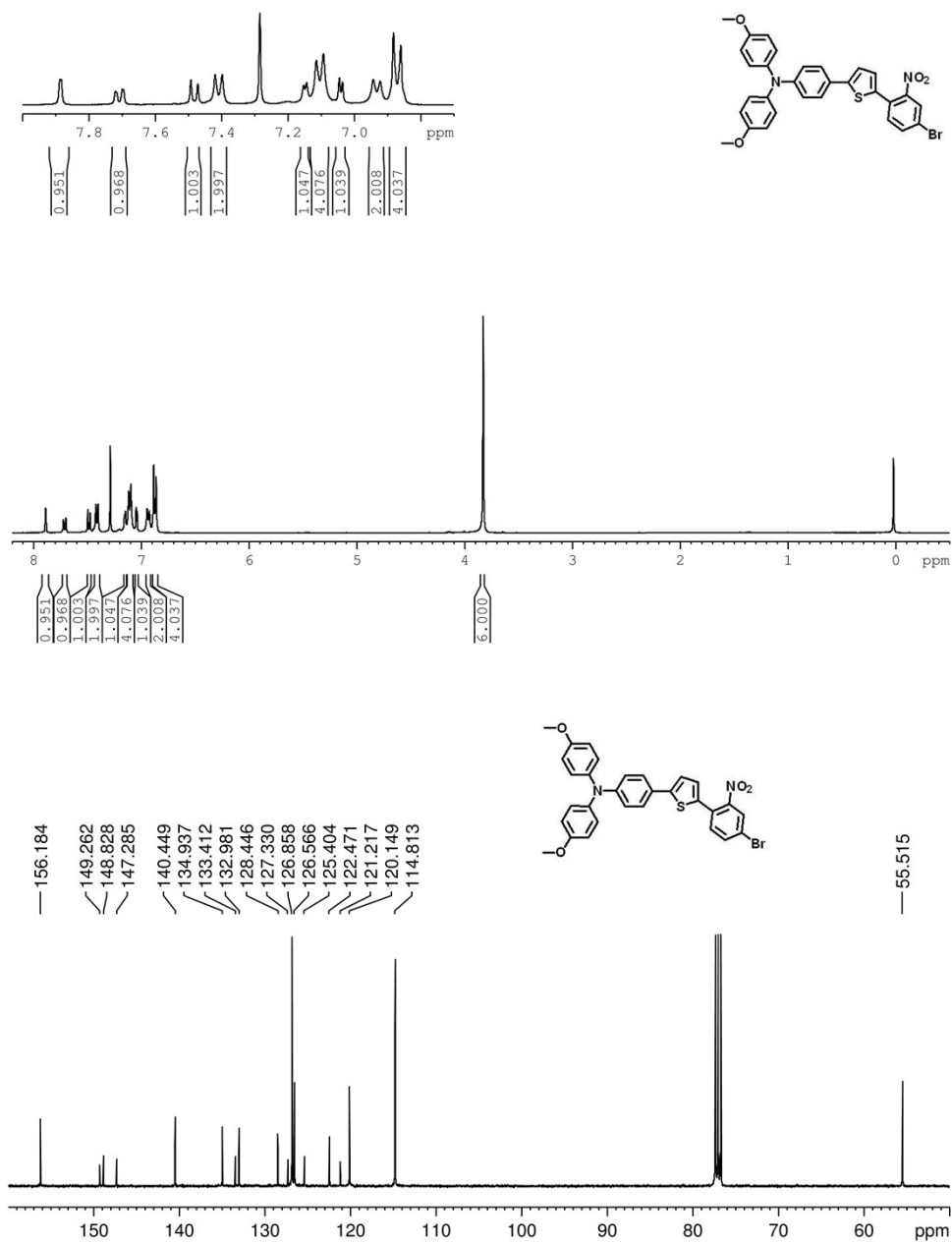


Fig. S1. ¹H (CDCl₃) and ¹³C NMR (CDCl₃) spectra of compound 2

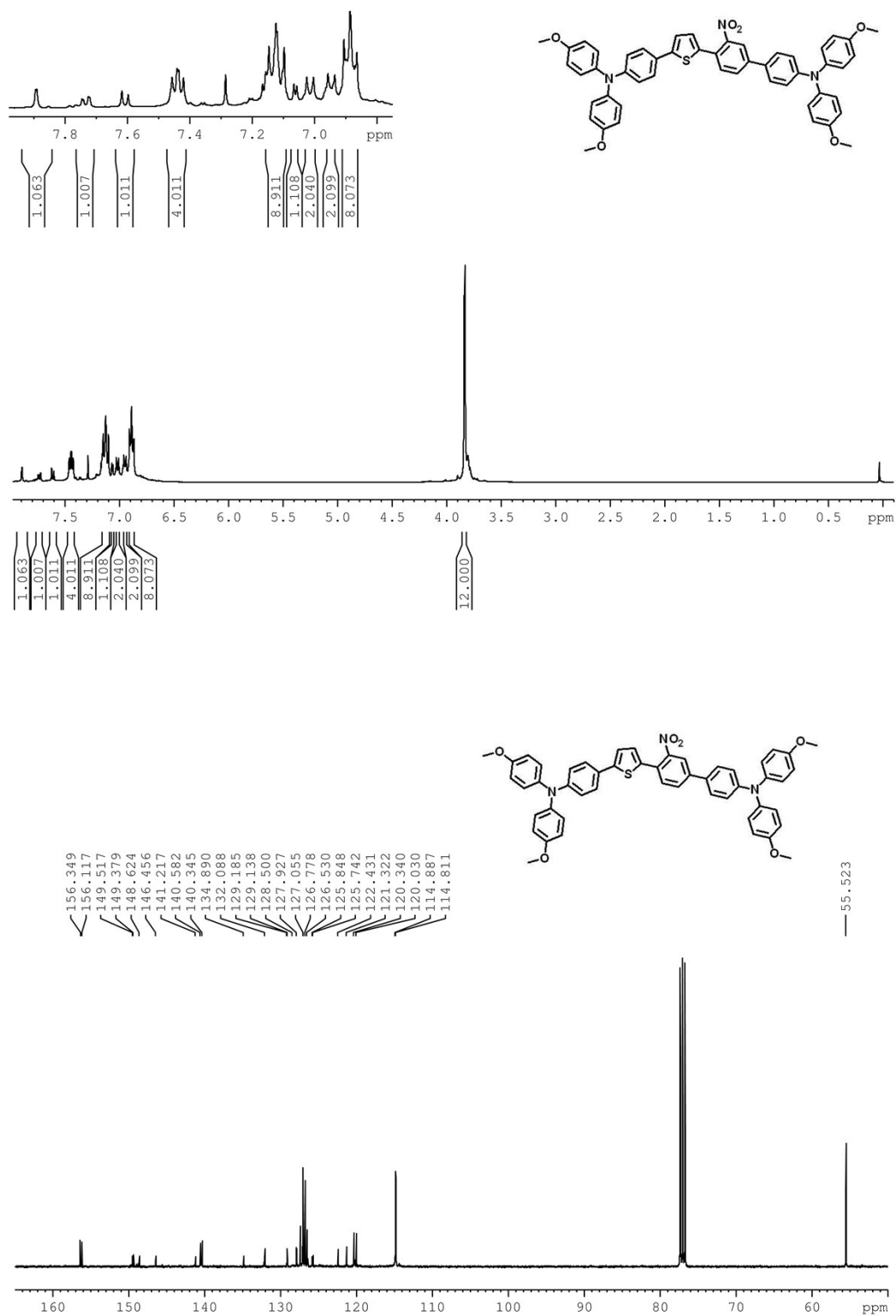


Fig. S2. ¹H (CDCl₃) and ¹³C NMR (CDCl₃) spectra of compound **3**

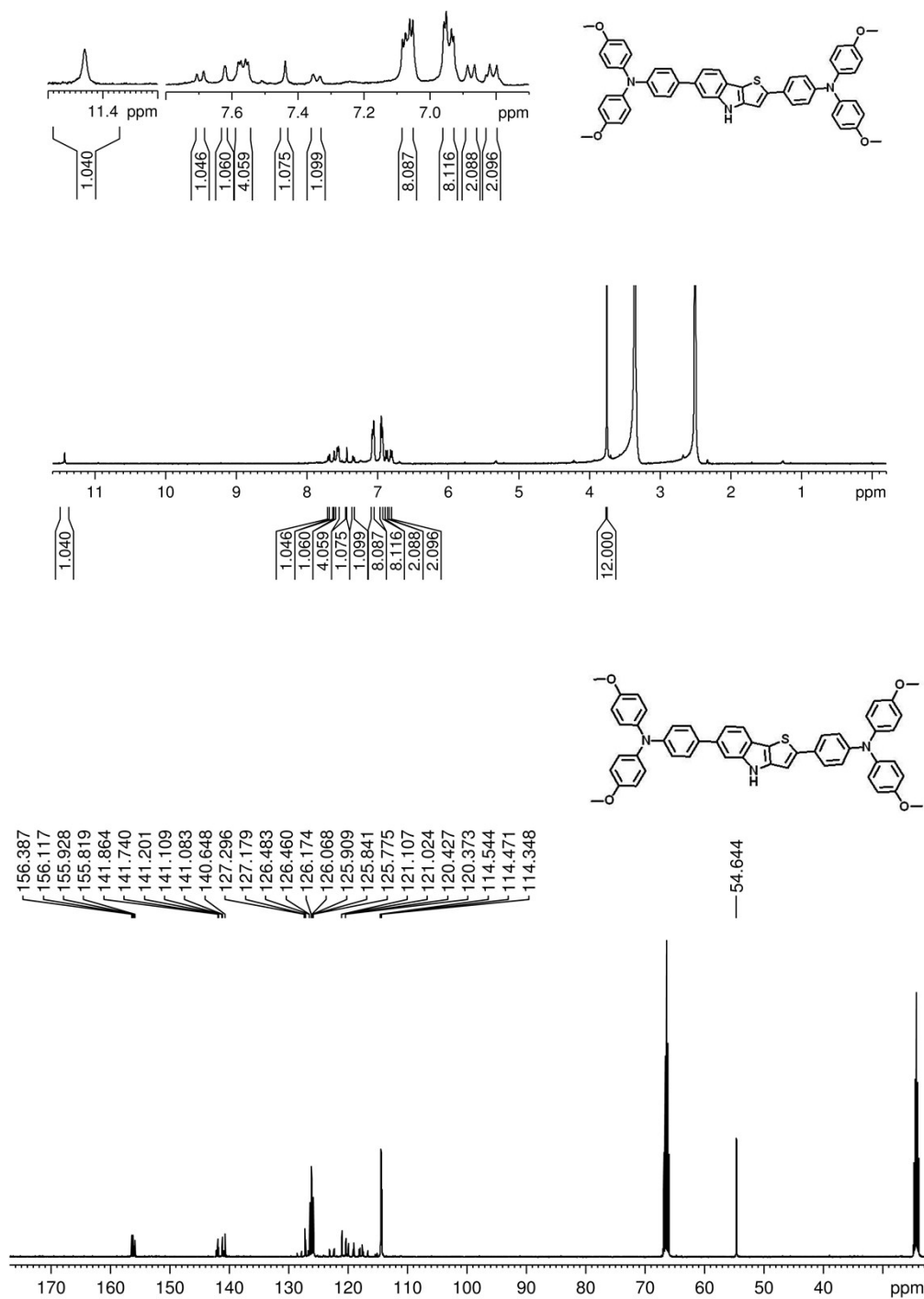


Fig. S3. ¹H (DMSO-*d*₆) and ¹³C NMR (THF-*d*₈) spectra of compound 4

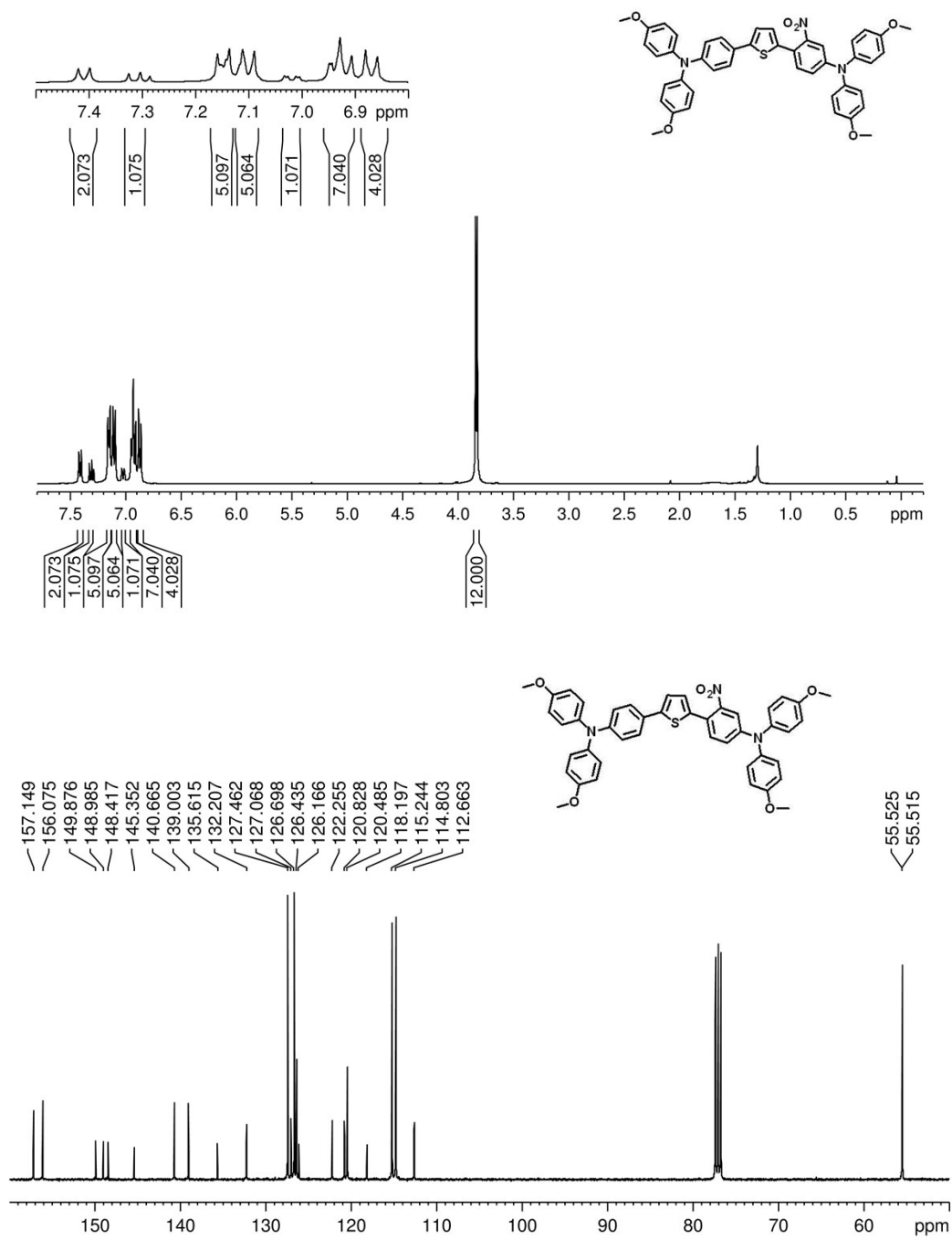


Fig. S4. ¹H (CDCl₃) and ¹³C NMR (CDCl₃) spectra of compound **6**

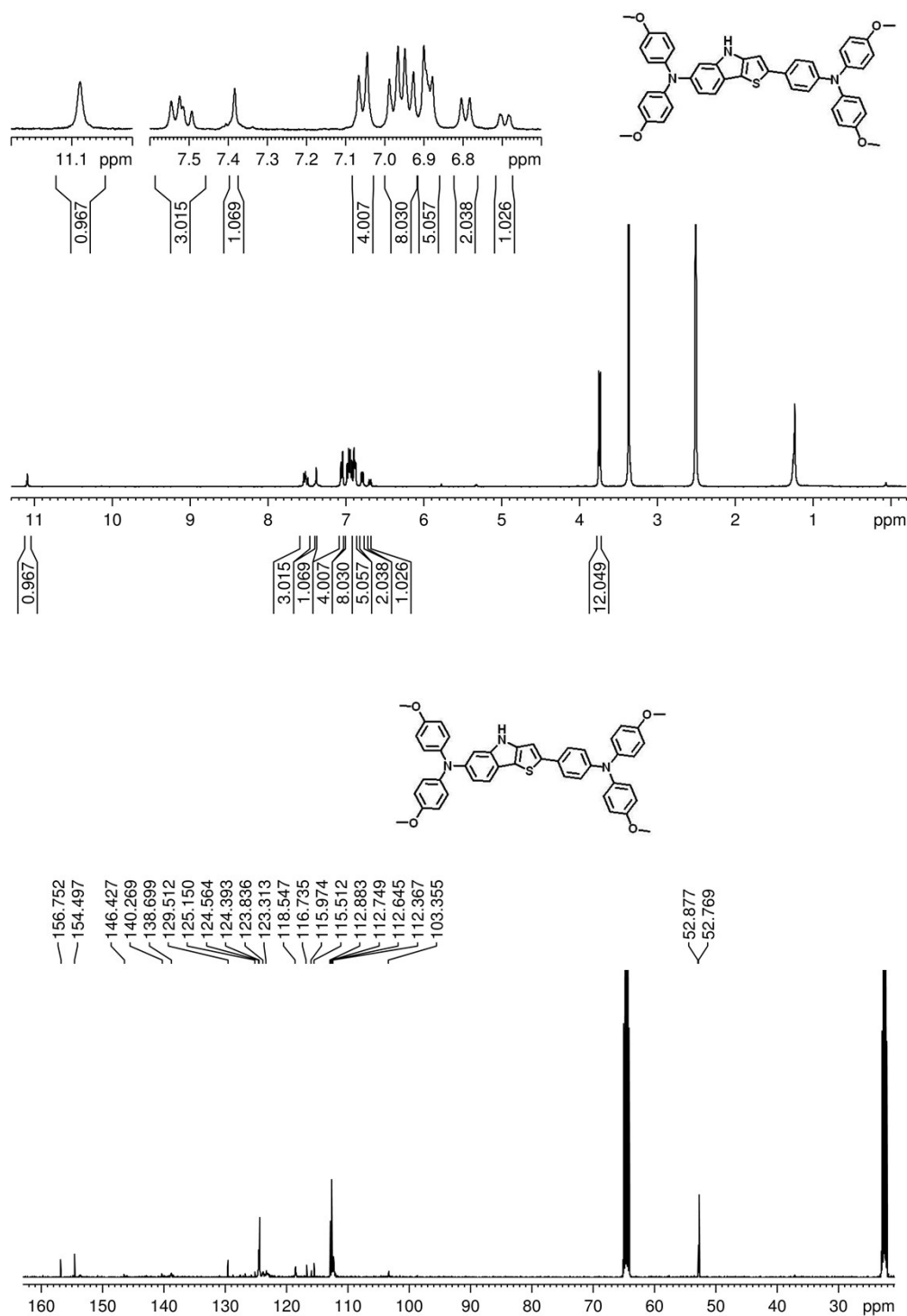


Fig. S5. ¹H (DMSO-*d*₆) and ¹³C NMR (THF-*d*₈) spectra of compound **7**

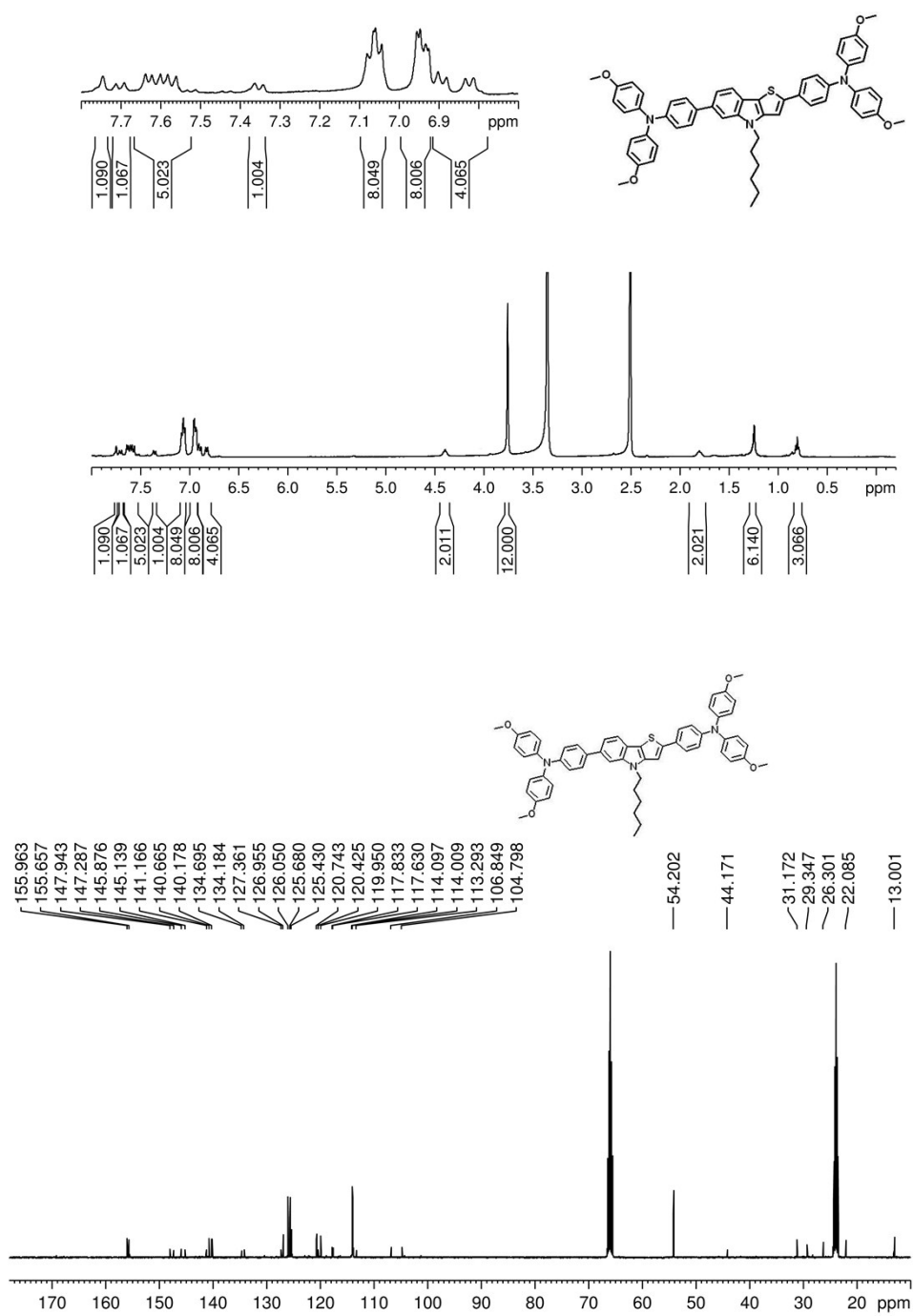


Fig. S6. ¹H (DMSO-*d*₆) and ¹³C NMR (THF-*d*₈) spectra of compound **M107**

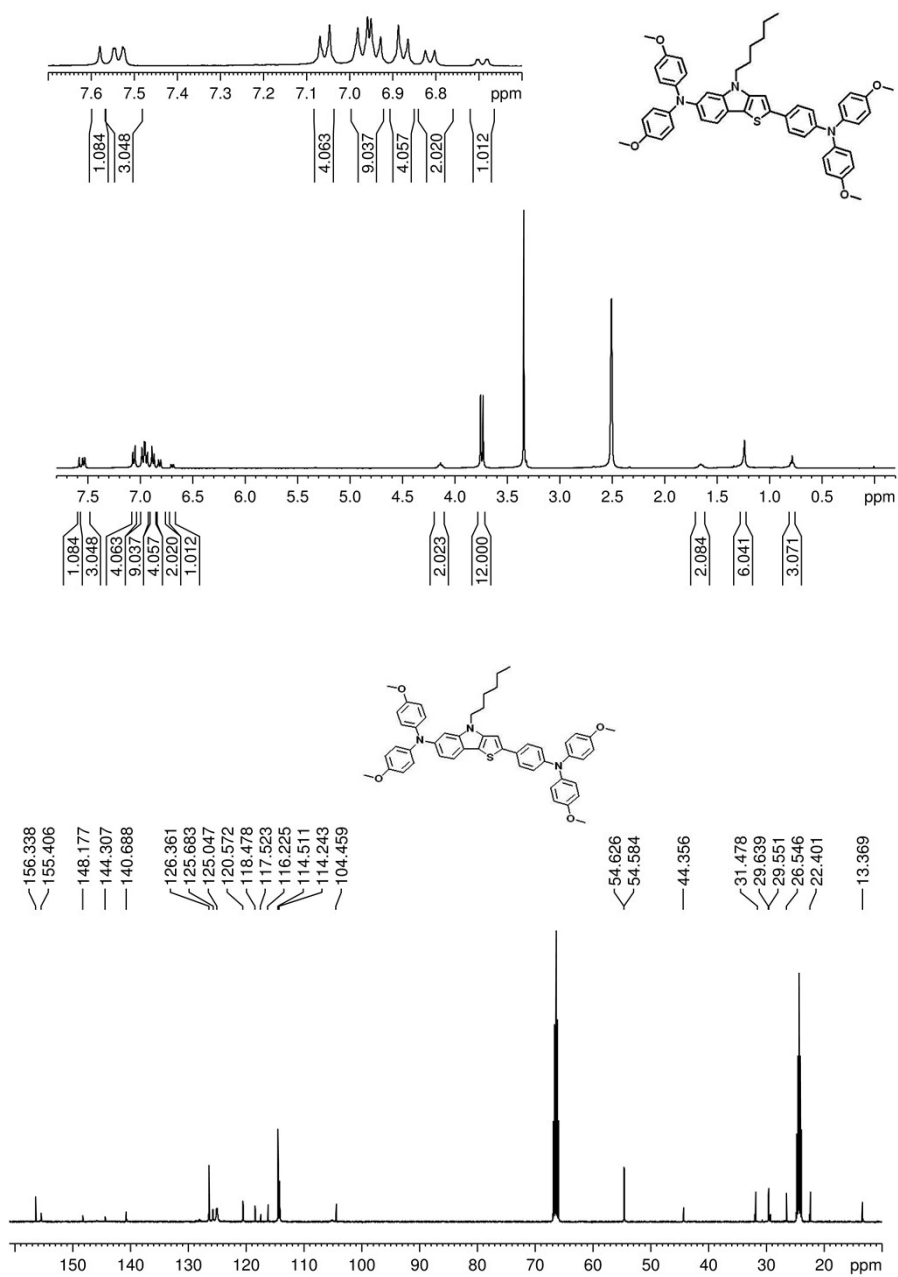


Fig. S7. ¹H (DMSO-*d*₆) and ¹³C NMR (THF-*d*₈) spectra of **M108**

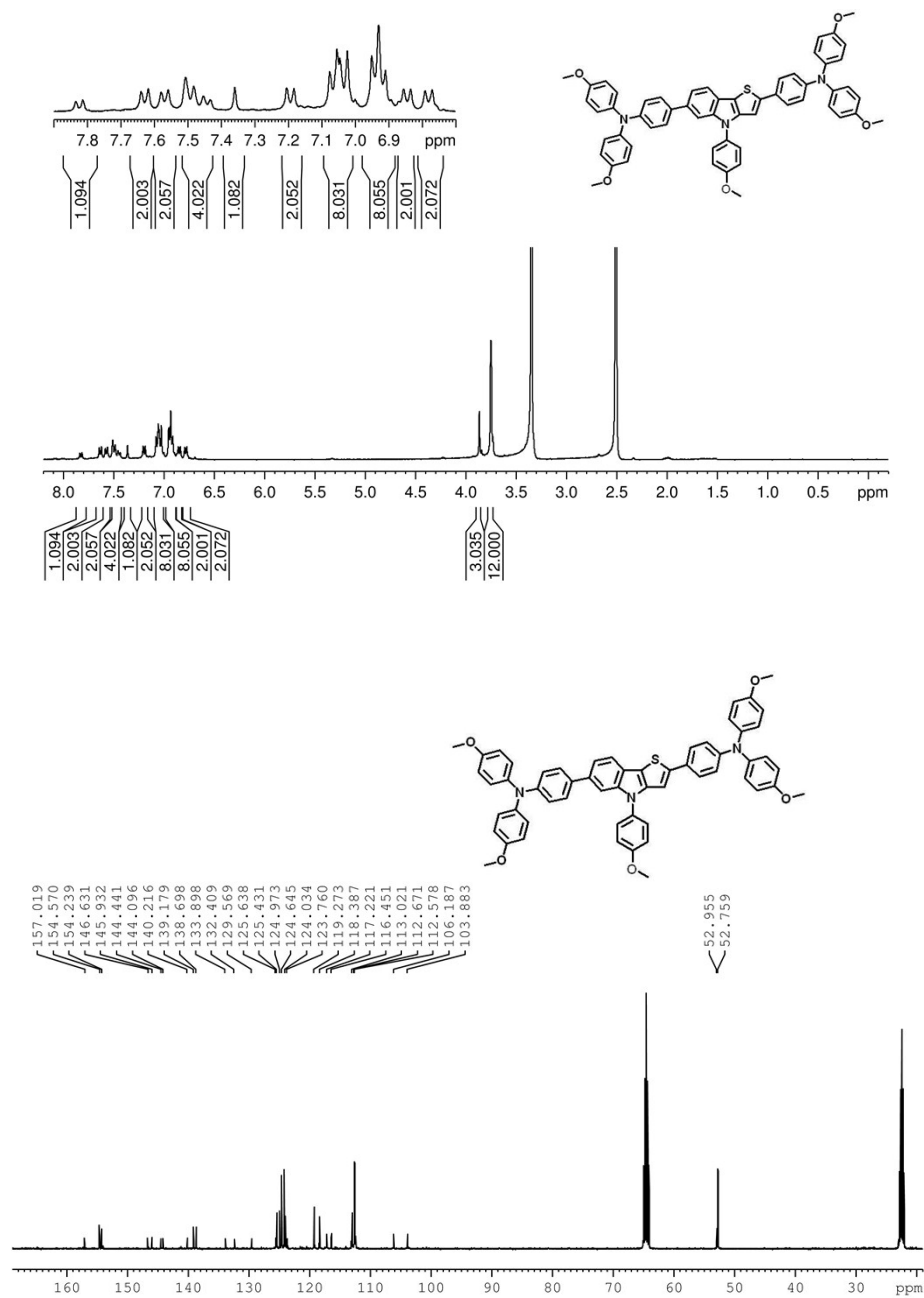


Fig. S8. ¹H (DMSO-*d*₆) and ¹³C NMR (THF-*d*₈) spectra of dye M109

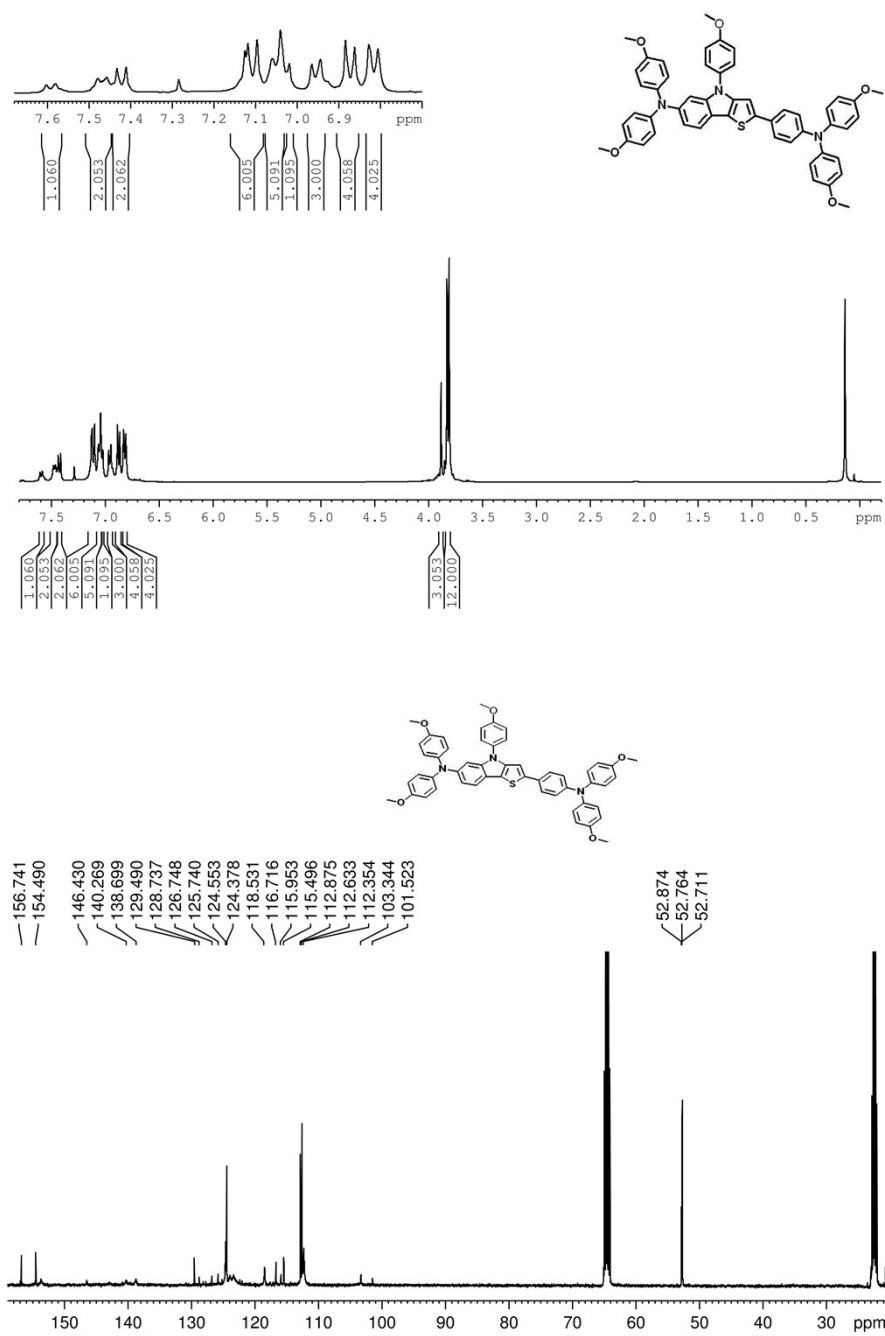


Fig. S9. ¹H (CDCl₃) and ¹³C NMR (THF-*d*₈) spectra of dye **M110**

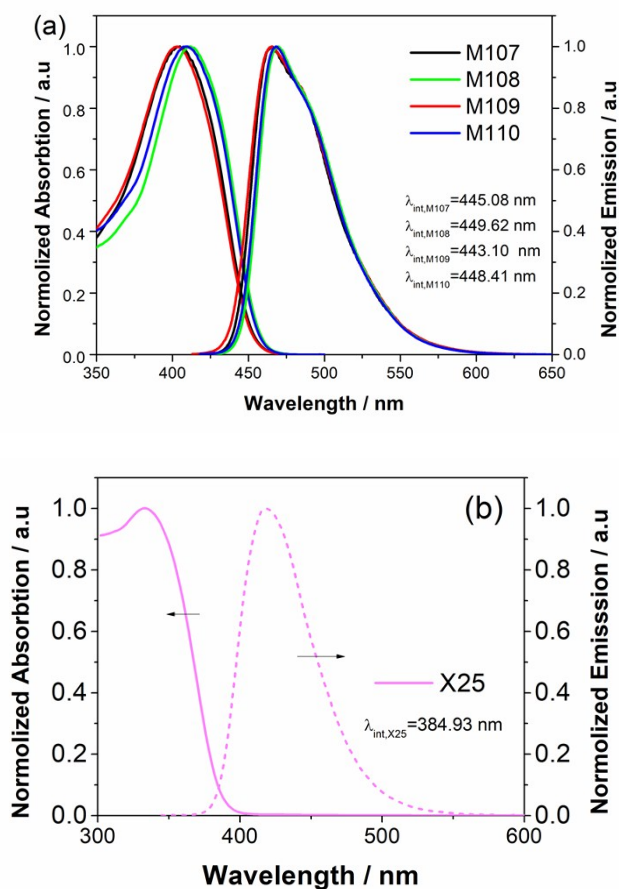


Fig. S10. Normalized absorption and emission spectra of M107-110 (a) and X25 (b).

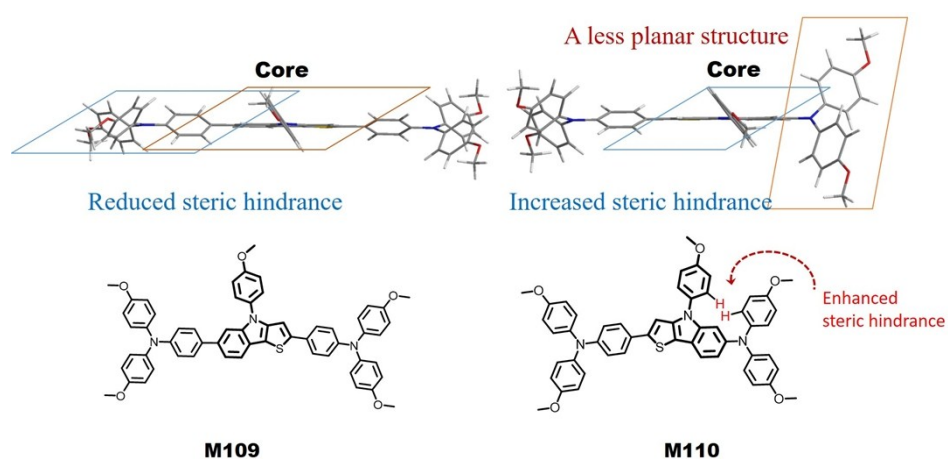


Fig. S11. The optimized ground-state molecular geometries and molecular structure of M109 and M110.

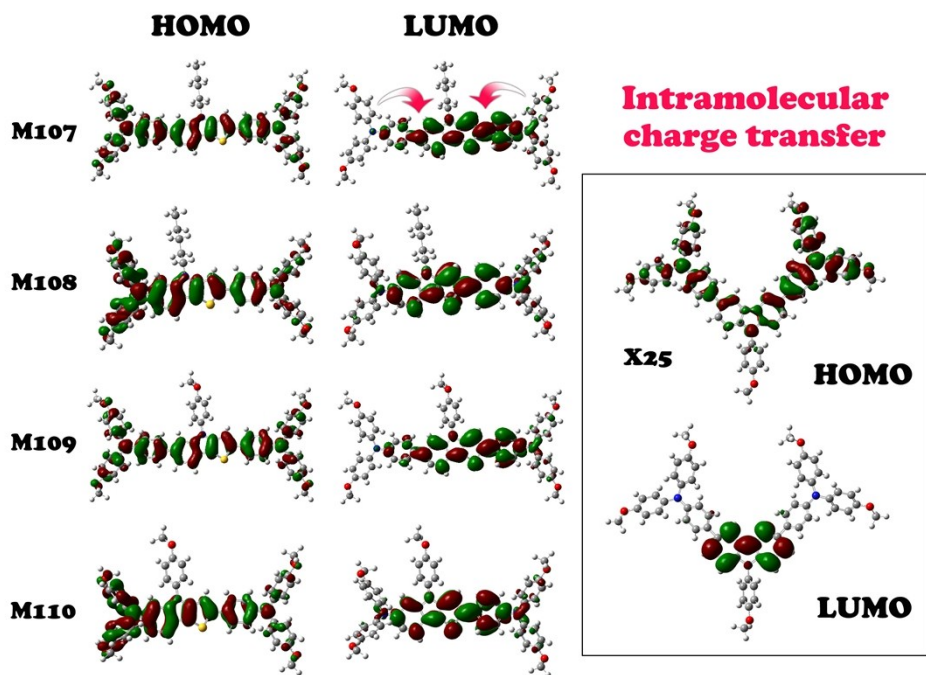


Fig. S12. The HOMO and LUMO of M107-110 and X25.

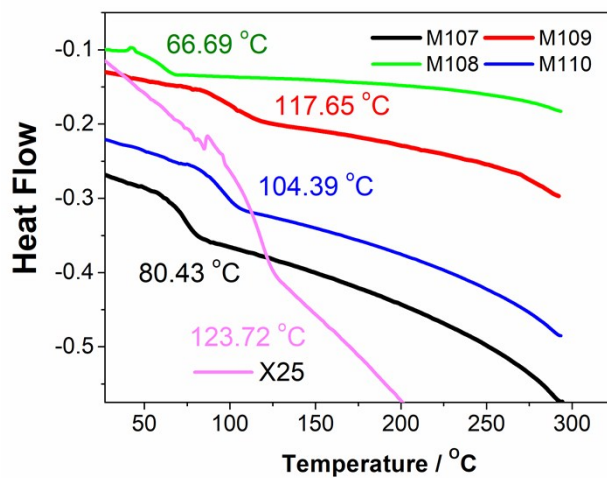


Fig. S13. The differential scanning calorimetry (DSC) of M107-110 and X25.

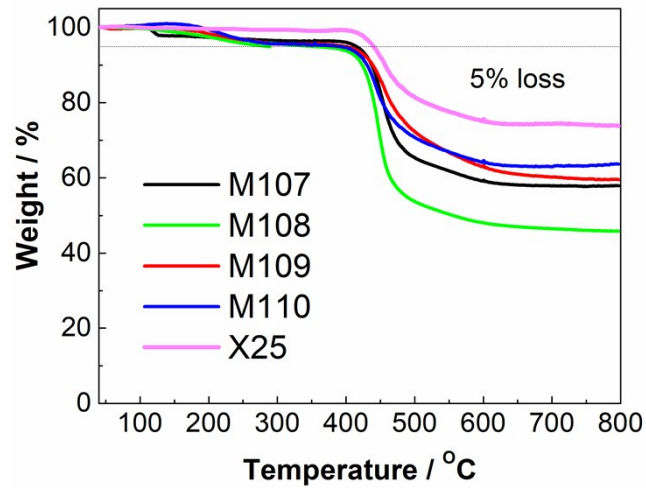


Fig. S14. The thermogravimetric analysis (TGA) of M107-110 and X25.

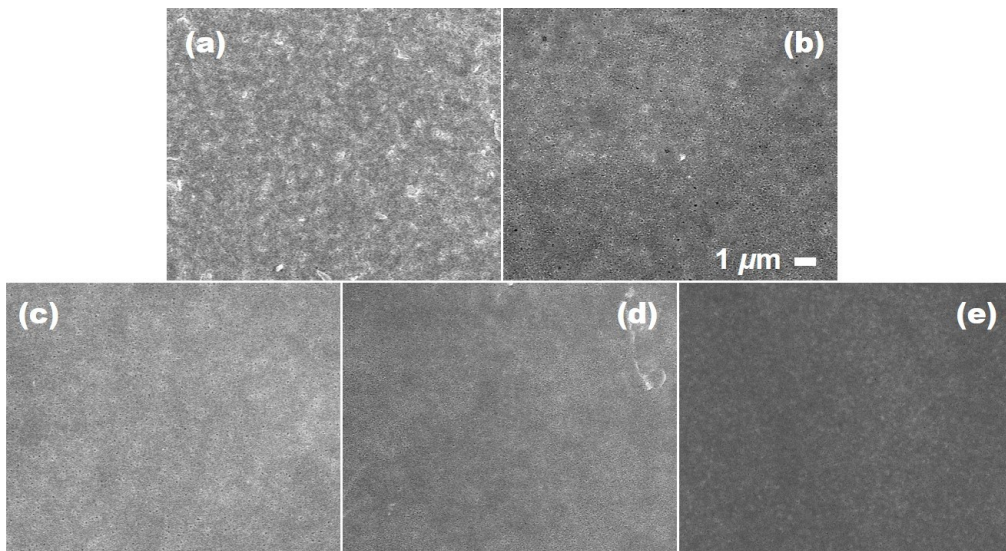


Fig. S15. SEM top-images of devices fabricated with the M107 (a), M108 (b), M109 (c), M110 (d) and X25 (e).

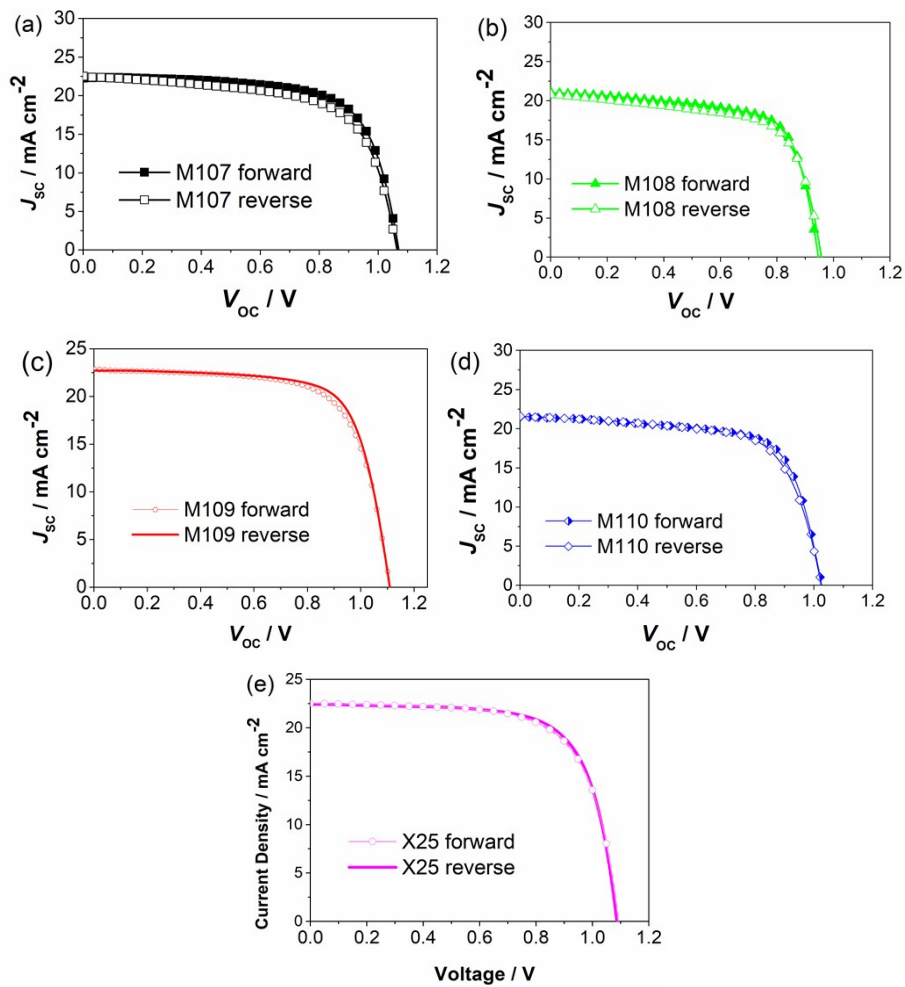


Fig. S16. J - V curves of the best devices for M107-110 and X25.

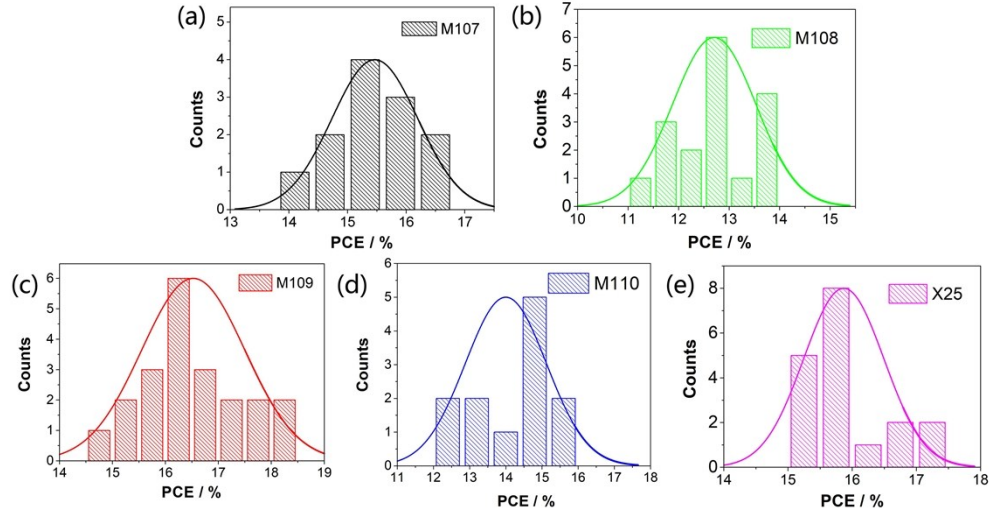


Fig. S17. Histogram of devices PCEs based on M107-110 and X25.

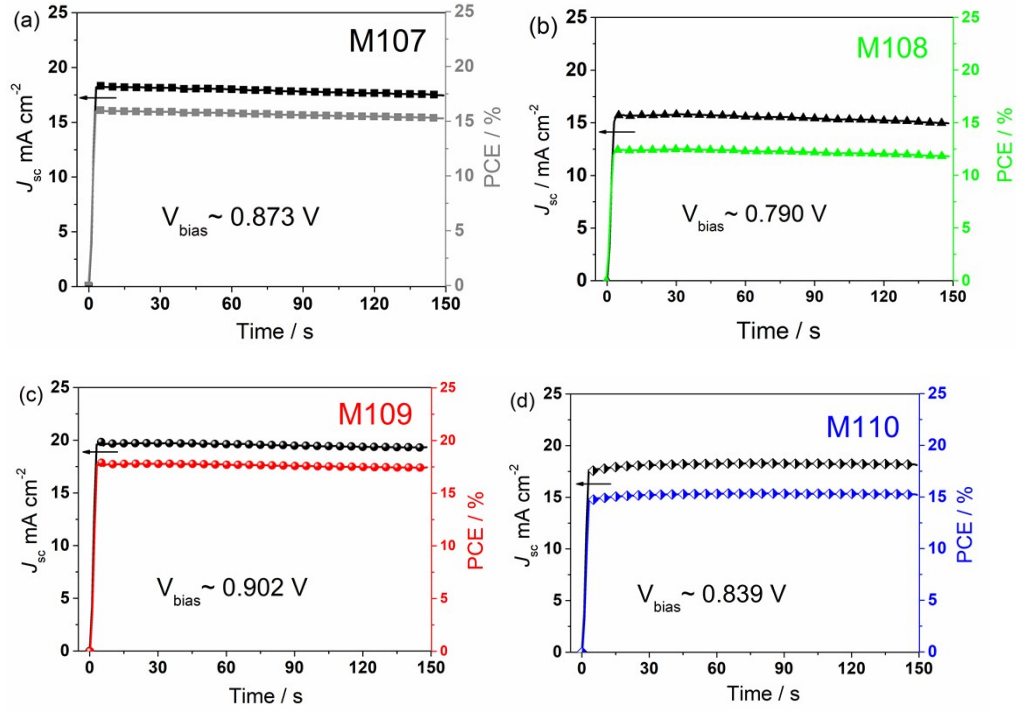


Fig. S18. The steady-state photocurrent and efficiency of the corresponding device at the maximum power point, M107 (a), M108 (b), M109 (c) and M110 (d).

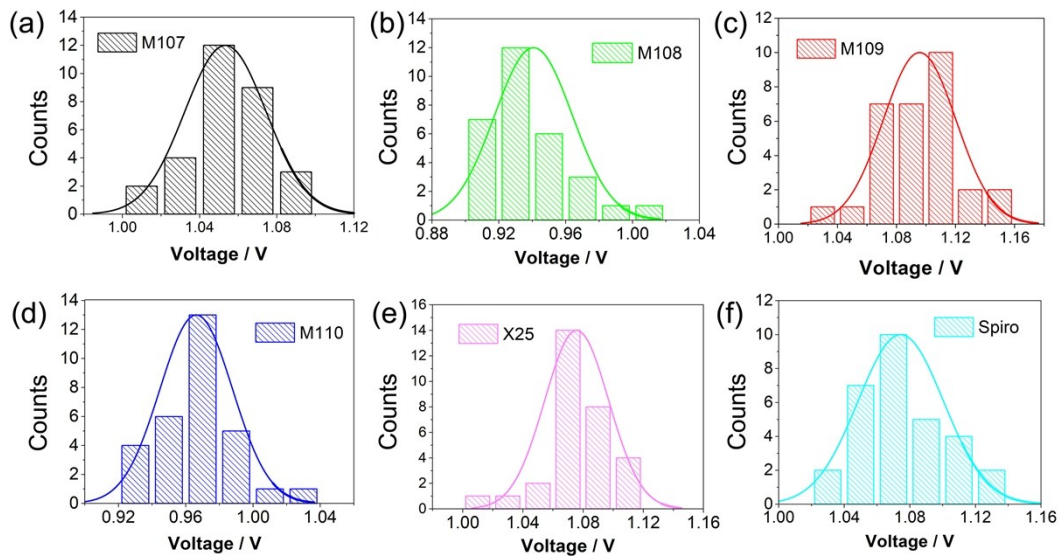


Fig. S19. Histogram of devices V_{OC} based on M107-110 and X25 (30 devices).

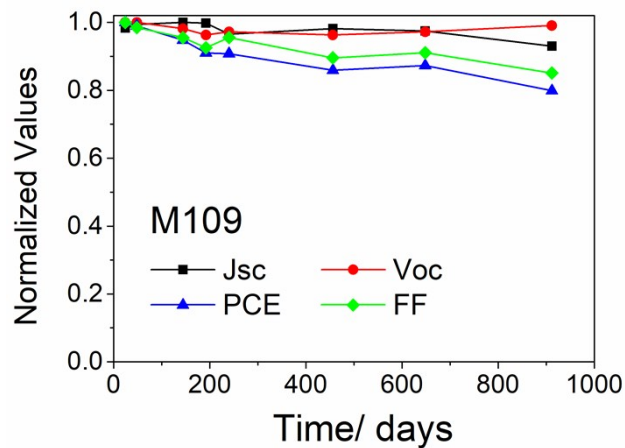


Fig. S20. Stability test of the M109 based PSC (with TBP and LiTFSI) in a glovebox under an inert atmosphere.

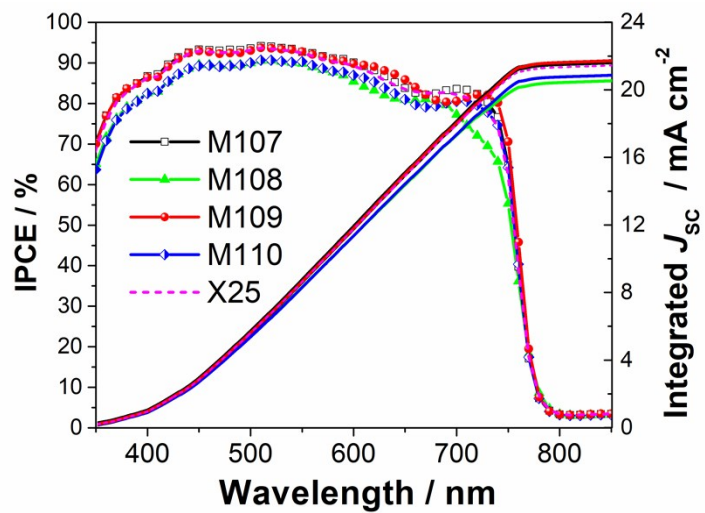


Fig. S21. IPCE spectra of the best PSCs based on M107-110 and X25.

References

- (1) Xu, B.; Sheibani, E.; Liu, P.; Zhang, J.; Tian, H.; Vlachopoulos, N.; Boschloo, G.; Kloo, L.; Hagfeldt, A.; Sun, L. Carbazole-Based Hole-Transport Materials for Efficient Solid-State Dye-Sensitized Solar Cells and Perovskite Solar Cells. *Adv. Mater.* **2014**, *26*, 6629-6634.
- (2) Bi, D.; Xu, B.; Gao, P.; Sun, L.; Grätzel, M.; Hagfeldt, A. Facile Synthesized Organic Hole Transporting Material for Perovskite Solar Cell with Efficiency of 19.8%. *Nano Energy* **2016**, *23*, 138-144.
- (3) M. J. Frisch, G. W. Trucks, H. B. Schlegel, G. E. Scuseria, M. A. Robb, J. R. Cheeseman, G. Scalmani, V. Barone, B. Mennucci, G. A. Petersson, H. Nakatsuji, M. Caricato, X. Li, H. P. Hratchian, A. F. Izmaylov, J. Bloino, G. Zheng, J. L. Sonnenberg, M. Hada, M. Ehara, K. Toyota, R. Fukuda, J. Hasegawa, M. Ishida, T. Nakajima, Y. Honda, O. Kitao, H. Nakai, T. Vreven, J. A. Montgomery, J. E. Peralta Jr., F. Ogliaro, M. Bearpark, J. J. Heyd, E. Brothers, K. N. Kudin, V. N. Staroverov, R. Kobayashi, J. Normand, K. Raghavachari, A. Rendell, J. C. Burant, S. S. Iyengar, J. Tomasi, M. Cossi, N. Rega, J. M. Millam, M. Klene, J. E. Knox, J. B. Cross, V. Bakken, C. Adamo, J. Jaramillo, R. Gomperts, R. E. Stratmann, O. Yazyev, A. J. Austin, R. Cammi, C. Pomelli, J. W. Ochterski, R. L. Martin, K. Morokuma, V. G. Zakrzewski, G. A. Voth, P. Salvador, J. J. Dannenberg, S. Dapprich, A. D. Daniels, O. Farkas, J. B. Foresman, J. V. Ortiz, J. Cioslowski and D. J. Fox, Gaussian 09, Revision D.01, Gaussian Inc., Wallingford, CT, 2009.
- (4) Jiang, Q.; Chu, Z.; Wang, P.; Yang, X.; Liu, H.; Wang, Y.; Yin, Z.; Wu, J.; Zhang,

X.; You, J., Planar-Structure Perovskite Solar Cells with Efficiency beyond 21. *Adv. Mater.* **2017**, *29*, 1703852.

(5) Saliba, M.; Matsui, T.; Seo, J.-Y.; Domanski, K.; Correa-Baena, J.-P.; Nazeeruddin, M. K.; Zakeeruddin, S. M.; Tress, W.; Abate, A.; Hagfeldt, A. Cesium-Containing Triple Cation Perovskite Solar Cells: Improved Stability, Reproducibility and High Efficiency. *Energy Environ. Sci.* **2016**, *9*, 1989-1997.